Journal of Solid and Fluid Mechanics (JSFM), 15(3): 13-16, 2025

Shahrood University of Technology

Journal of Solid and Fluid Mechanics (JSFM)

DOI: 10.22044/jsfm.2025.16052.3958

Manufacturing Engineering of Iran

A Computational Analysis of the Aerodynamic Behaviors of Low-Speed Conventional Airfoils

Hossein Ansarian[1*], Alireza Davari[2]

[1]Aerospace Research Group, Malek Ashtar University of Technology, Tehran, Iran
[2] Assoc. Prof., Department of Engineering, Science and Research Branch, Islamic Azad University, Tehran, Iran
*Corresponding author: hossein.ansarian@gmail.com

Received: 04/13/2025 Revised: 07/19/2025 Accepted: 07/29/2025

Abstract

This paper investigates the aerodynamic characteristics of NACA airfoils 0012, 0015, and 4415 in the low Reynolds number range of 500 to 2000. High-resolution, two-dimensional simulations of incompressible, unsteady flow were conducted using a sharp-interface immersed boundary method and the Navier–Stokes equations. The goal of this study is to present a database of variations in aerodynamic coefficients, Strouhal numbers, and center of pressure as functions of Reynolds number, angle of attack, and airfoil shape. The results reveal that low Reynolds number flows exhibit significant complexity due to phenomena such as Karman vortex shedding and leading-edge vortex (LEV) formation and shedding. These behaviors lead to large and rapid changes in aerodynamic coefficients with varying angles of attack. The effect of airfoil shape is primarily observed in the lift-to-drag ratio and center of pressure, with the NACA 4415 airfoil demonstrating the highest aerodynamic performance. Comparison of simulation results with available experimental data at both low and high Reynolds numbers confirms the validity of the employed numerical model. This database serves as a reference for designing small aircraft, unmanned aerial vehicles, and bio-inspired flight systems. Additionally, the obtained data can aid in improving and validating computational models.

Keywords: Aerodynamic Characteristics, NACA Airfoils, Low Reynolds Number, Incompressible Flow.

1. Introduction

The aerodynamic characteristics of airfoils at low Reynolds numbers differ significantly from those at high Reynolds numbers, which are typically observed in conventional aircraft. Due to recent interest in unmanned aerial vehicles and micro air vehicles, this low-Reynolds-number behavior has attracted considerable scientific and practical attention. However, the available data in the literature on low-Reynolds-number aerodynamics remain limited [1,2].

This distinct behavior arises from increased viscous effects and laminar flow conditions, leading to thicker boundary layers and laminar separation. An initial set of measurements in the range of $Re \approx 5\times10^4–5\times10^5$ was conducted by Selig et al. [3]. However, few studies have examined airfoil flows at $Re \approx 10^3$ due to the experimental challenges of generating such flows. Numerical studies on stationary airfoils at low Reynolds numbers have often employed steady-state models, neglecting time-dependent phenomena such as vortex shedding [4]. Kurtulus [5] investigated the flow around a NACA 0012 airfoil for different angles of attack at $Re = 10^3$ using unsteady simulations. Liu et al. [6] investigated flow separation for the same airfoil at the same Reynolds number. However, these studies were limited to a single airfoil shape and Reynolds number.

In the present study, we report simulation results for low-Reynolds-number flows ($500 \leq Re \leq 2000$) over three different airfoils. The objective is to establish a comprehensive database of key aerodynamic parameters as functions of Reynolds number, angle of attack, and airfoil geometry.

2. Computational Method

The flow was simulated using an immersed boundary method with a sharp interface, developed and validated by Mittal et al. [7]. The incompressible unsteady Navier-Stokes equations were solved by a fractional-step method, and a geometric multigrid approach was used to solve the pressure Poisson equation. Spatial derivative terms were computed using the finite difference discretization with a second-order accuracy, and a second-order Adams-Bashforth scheme was used for temporal integration. The computed lift coefficients and lift oscillation frequencies were compared with published data (Fig. 1), showing good agreement.

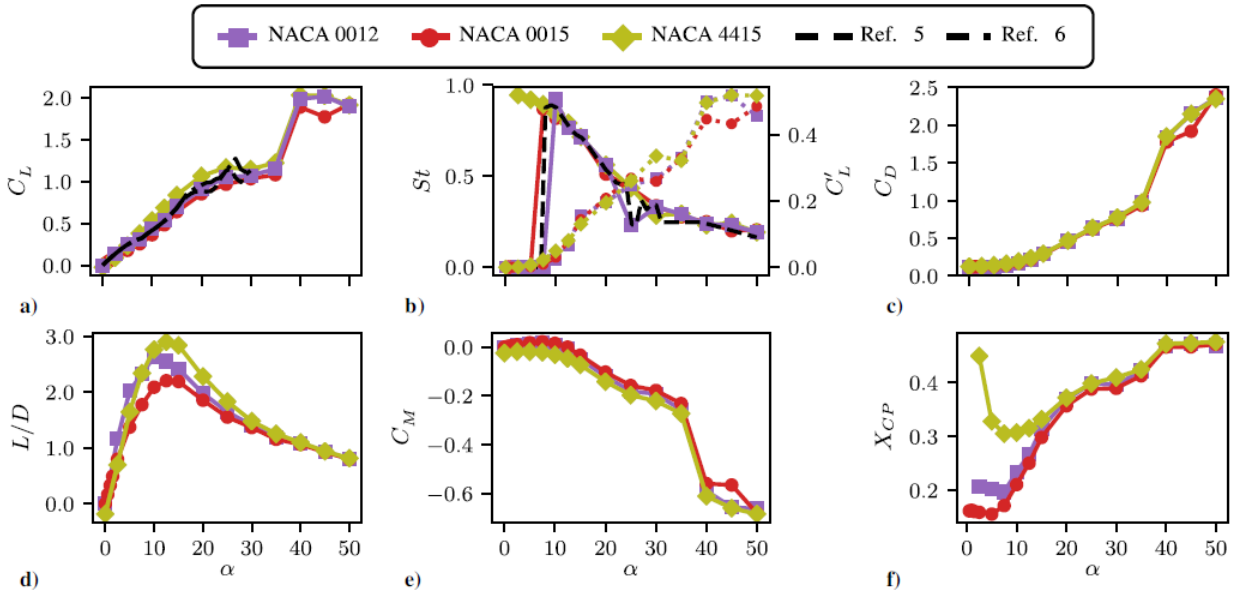

Figure 1. Aerodynamic characteristics of the three airfoils at Re = 1000

3. Results and Discussion

The airfoils examined in this study include the NACA 0012, 0015, and 4415, placed in a computational domain of size 20C×18C. A non-conformal structured grid with 480×448 nodes was used. Grid independence was verified by simulating flow over the NACA 0015 airfoil at Re = 2000, evaluating the mean and root-mean-square values of lift and pitching moment coefficients for grid resolutions of 320×384, 448×480, and 544×544. Convergence was achieved with the second grid resolution.

3.1. Flow Regimes

Flow simulations at various angles of attack for the NACA 0015 airfoil at Re = 10^3 (Fig. 2) reveal that as the angle of attack exceeds the static stall angle, the steady wake transforms to a Karman vortex street and eventually to a flow dominated by leading-edge vortices. A steady regime before vortex shedding is observed at $\alpha = 5°$. At $\alpha = 15°$, Karman vortex shedding causes periodic oscillations in C_L and C_M. At $\alpha = 25°$, the time histories of C_L and C_M exhibit both low- and high-frequency components due to single and paired vortex shedding modes. The high-frequency component arises from the Karman shedding, while the generation and shedding of leading-edge vortices induce low-frequency oscillations. At $\alpha = 40°$, low-frequency shedding of a large leading-edge vortex and a small trailing-edge vortex dominate. The time-varying coefficients in this regime exhibit quasi-periodic behavior with random fluctuations.

3.2. Reynolds Number Effects

Figure 3 compares the calculated aerodynamic coefficients for the NACA 0015 airfoil at three different Reynolds numbers as functions of α, alongside experimental measurements [2] at Re = 7×10^5. At low angles of attack, the mean C_L values for the three Reynolds numbers are similar, with a lift slope approximately half the theoretical value (2π) and comparable to that at Re = 7×10^5. The mean value of the lift coefficient increases in a monotonic way for Re = 500 and 1000, while a partial stall occurs for Re = 2000 in the range $20° \leq \alpha \leq 25°$. However, none exhibit the deep stall observed at high Reynolds numbers. Unlike high-Reynolds-number behavior, all three simulations show a noticeable growth in mean C_L at $\alpha \geq 35°$, attributed to leading-edge vortex formation and shedding. The magnitude of this jump increases with Reynolds number.

At low angles, the Strouhal number is zero due to steady flow. As the angle of attack increases, a sharp rise in St marks the onset of unsteady vortex shedding, followed by a gradual decline. The transition to unsteadiness is observed within $\alpha \approx 12.5°$ for Re = 500 and $\alpha \approx 5°$ for Re = 2000. The intensity of lift oscillations, represented by the standard deviation C'_L, increases uniformly with angle for Re = 500 and 1000, but Re = 2000 exhibits complex, non-monotonic behavior.

The drag coefficient shows no notable trends except for a sharp rise at $\alpha > 20°$ for the two higher Reynolds numbers. The drag at these conditions exceeds that at high Reynolds numbers. The maximum C_L/C_D is seen at $\alpha \approx 15°$ for Re = 500 and $\alpha \approx 10°$ for Re = 2000, with lower values than those at higher Reynolds numbers.

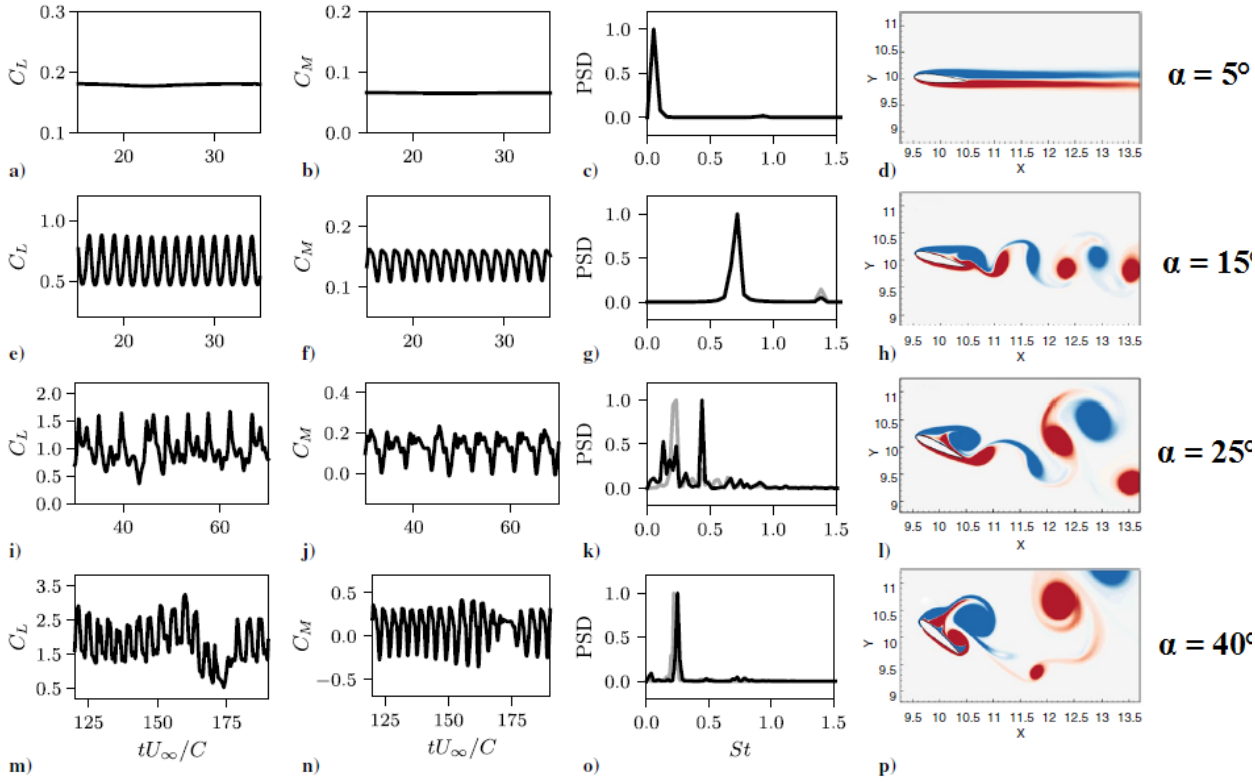

Figure 2. Lift and moment coefficients and vorticity contours of the NACA 0015 airfoils at Re = 1000 and different angles of attack

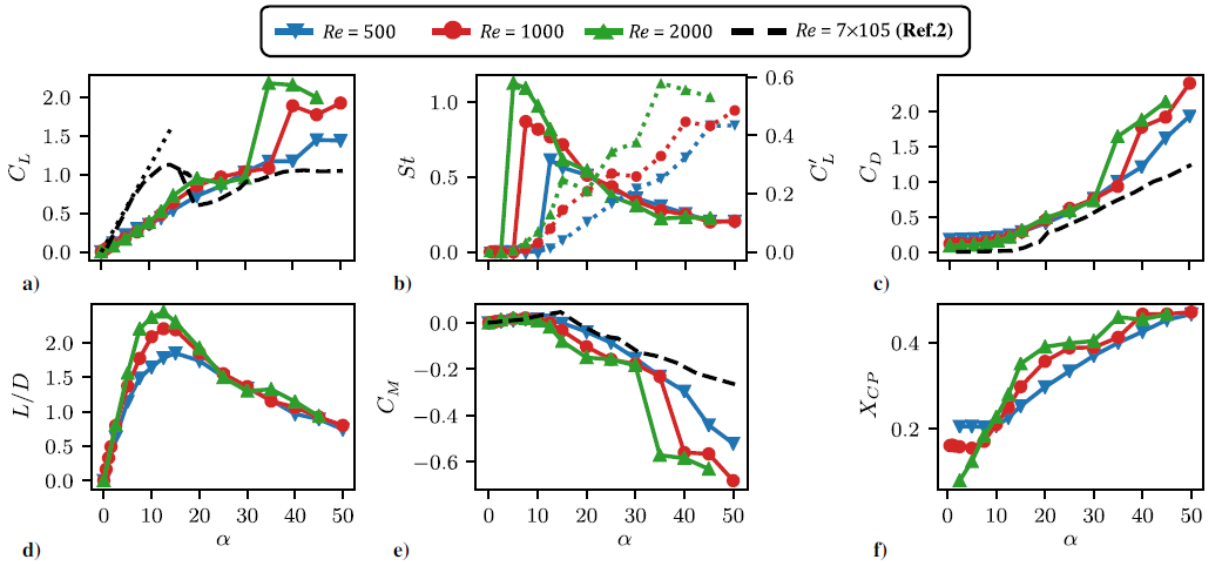

Figure 3. Aerodynamic characteristics of the NACA 0015 airfoils at different Reynolds numbers compared with the experimental data

At small angles of attack, the pitching moment is near zero and varies minimally with α. Its magnitude increases with Reynolds number at high angles and remains negative for α > 10°, reflecting a rearward shift in the center of pressure. At low Reynolds numbers, the center of pressure remains fixed at small angles but shifts further downstream compared to higher Reynolds numbers. As the angle of attack increases, it moves aft, reaching near mid-chord by α = 50°.

3.3. Airfoil Shape Effects

It is observed in Fig. 1 that the NACA 4415 airfoil generates a small negative lift at α = 0°, which increases more rapidly with angle than the other airfoils, resulting in higher mean lift at moderate angles. The NACA 4415 also achieves the highest

C_L/C_D. Its center of pressure differs from the other two airfoils at $\alpha < 15°$.

4. Conclusions

In this study, high-resolution unsteady incompressible flow simulations were conducted to examine the aerodynamic performance of three NACA airfoils at Reynolds numbers of 500, 1000, and 2000, across angles of attack ranging from 0° to 50°. Despite the flow's low Reynolds number and laminar, the flow behavior exhibits significant complexity due to various flow phenomena such as leading-edge vortex formation and shedding, as well as Karman vortex shedding. This complexity results in large and fast variations in evaluated aerodynamic parameters with changing angle of attack. The effect of airfoil shape is mostly observed in the lift-to-drag ratio and the location of the center of pressure.

5. References

[1] Abbott IH, Von Doenhoff AE (1959) *Theory of wing sections, including a summary of airfoil data*. Dover Publ., New York, Appendix IV.

[2] Sheldahl RE, Klimas PC (1981) Aerodynamic characteristics of seven symmetrical airfoil sections through 180-degree angle of attack for use in aerodynamic analysis of vertical axis wind turbines. Sandia National Laboratories (SNL) Tech. Rept. SAND80-2114, Albuquerque, NM, and Livermore, CA.

[3] Selig M, Guglielmo J, Broeren A, et al. (1995) *Summary of low-speed airfoil data*. Vol. 1, SoarTech Publ., Virginia Beach, VA, Chap. 4.

[4] Mateescu D, Abdo M (2010) Analysis of flows past airfoils at very low Reynolds numbers. *Proc Inst Mech Eng G J Aerosp Eng* 224(7):757–775.

[5] Kurtulus DF (2015) On the unsteady behavior of the flow around NACA 0012 airfoil with steady external conditions at Re = 1000. *Int J Micro Air Veh* 7(3):301–326.

[6] Liu Y, Li K, Zhang J, Wang H, Liu L (2012) Numerical bifurcation analysis of static stall of airfoil and dynamic stall under unsteady perturbation. *Commun Nonlinear Sci Numer Simul* 17(8):3427–3434.

[7] Mittal R, Dong H, Bozkurttas M, et al. (2008) A versatile sharp interface immersed boundary method for incompressible flows with complex boundaries. *J Comput Phys* 227(10):4825–4852.